J Mater Sci: Mater Med (2008) 19:1935–1943
DOI 10.1007/s10856-007-3273-5

The influence of surface topography on wear debris generation at the cement/bone interface under cyclic loading

Kirk A. Stoffel · Dongliang T. Yang · Dwayne Arola

Received: 7 December 2006 / Accepted: 5 September 2007 / Published online: 13 October 2007

Abstract The long-term success of a total joint replacement can be undermined by loosening of the implant, generation of wear debris or a combination of both factors. In the present study the influence of the surface morphologies of the bone and cement mantle on loosening of cemented total joint replacements (THJRs) and development of wear debris were studied. Model cemented THJR specimens were prepared in which the femoral canal was textured using specific cutting tools. The specimens were subjected to cyclic loads inducing pure shear fatigue of the cement/bone interface. Changes in both the femoral canal and cement mantle resulting from fatigue were quantified in terms of the surface topography and the volume of wear debris. Loosening occurred with cyclic loading due to degradation of the cement and bone and resulted in the development of cement and bone particles. There was no correlation between the fatigue strength of the interfaces and the volume of wear debris. In general, the change in surface topography of the cement mantle with fatigue decreased with increasing volume of cement interdigitation. Femoral canal surfaces with symmetric profile height distribution (i.e., Gaussian surfaces) resulted in the lowest volume of generated debris.

1 Introduction

Despite many improvements in surgical techniques and implant designs, total hip join replacement (THJR) failures are not uncommon, particularly in some implant designs. In cemented systems, loosening of the femoral component is the most frequent cause of failure [1]. Despite recognition as both an important and persistent problem, the mechanisms responsible for initiation and progression of loosening have not yet been clearly identified.

Clinical evidence suggests that the incidence of femoral component loosening in cemented THJRs most frequently occurs along the cement/bone interface [e.g., 2, 3]. Loosening may result from mechanical and/or biological factors. Mechanical failures arise from cyclic loading and initiation of damage in the cement that culminates in fatigue failure [4, 5]. Indeed, particulate cement debris resulting from micromotion and degradation of the cement mantle is often found in the connective tissue around failed implants [6, 7]. Cement particles have also been implicated as a cause for bone resorption around cemented devices [8, 9] and play a role in the etiology of osteolysis around even well fixed cemented femoral components [10]. Both Jasty et al. [11] and Goetz et al. [12] showed that osteolytic induced bone resorption could occur without substantial loosening of the implant. As the fate of a THJR is generally defined very early (i.e., within 2 years [13–15] or even the first 6 months post-operative [16]), it would appear unlikely that wear particles and cement debris are responsible for the initiation of loosening [17]. However, the transition between early migration and clinical failure is unclear and cement debris may play a role in the early progression of loosening of the prosthesis.

Previous studies have established that the surface texture of the prosthesis and the bone contribute to the integrity of the cement/prosthesis and cement/bone interfaces [18–23]. An increase in surface roughness fosters mechanical interlock, thereby reducing the potential for loosening. Heiple et al. [24] reported that the shear strength of the

K. A. Stoffel · D. T. Yang · D. Arola (✉)
Department of Mechanical Engineering, University of Maryland Baltimore County, 1000 Hilltop Circle, Baltimore, MD 21250, USA
e-mail: darola@umbc.edu

cement/bone interface was improved by texturing the femoral canal to enhance interdigitation. Similarly, the fatigue strength of the cement/bone interface was recently shown to increase with surface roughness of the bone and interdigitation [25]. If cement debris develops as a result of micromotion, improvements in the cement/bone interface may help minimize the development of debris. Yet, no study has quantified the influence of bone surface texture on changes to the cement/bone interface that arise with cyclic loading and/or loosening.

In the present study, model THJR specimens were prepared and subjected to cyclic loading. Specifically, designed cutting tools were used to texture the femoral canals prior to cementing and the surface topography at the cement/bone interface was examined before and after cyclic loading. The objectives of the present study were to evaluate the influence of bone surface topography and interdigitation of cement on loosening of the cement/bone interface and to quantify the volume of wear debris generated and changes in the interface morphology as a result of fatigue.

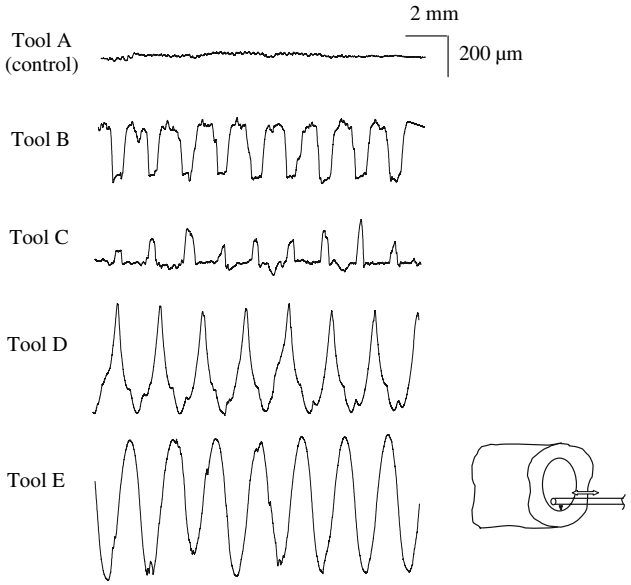

Fig. 1 Surface profiles of the femoral canal resulting from use of the five different cutting tools. The profiles have been acquired parallel to the canal. Note the difference in vertical and horizontal scales

2 Materials and methods

Bovine rear femurs were acquired from a commercial slaughterhouse within 24 h of slaughter. Transverse sections of 25 mm length and adequate wall thickness ($t \geq 5$ mm) and canal diameter ($d \leq 25$ mm) were obtained from the mid-diaphyseal region of the femurs. The femoral canal of each section was enlarged to 30 mm, and then expanded to a final diameter of 31.7 mm using one of five different cutting tools. The bone was maintained in a calcium-buffered saline solution [26] at room temperature throughout these procedures. One of these tools (designated Tool A) served as the control and was used to impart a surface roughness similar to that resulting from use of an endosteal broach. Four additional tools (designated Tools B–E) were designed to impart different canal surface textures. All five tools were used with rotation and resulted in the primary topographical lay extending along the circumferential direction. Surface profiles of the bone resulting from preparation with each tool were obtained parallel to the axis of the femoral canal (perpendicular to the lay) as shown in Fig. 1.

Model THJR specimens were prepared from the sections of bone to simulate the femoral side (Fig. 2). Each specimen consisted of a model implant cemented within a section of the prepared femur. The model implant "stem" consisted of a 25.4 mm diameter cylindrical section of Ti6Al4V. The stem and canal diameters resulted in a cement mantle thickness of approximately 3 mm. The surface of the stems was textured using a knurling tool to minimize failure of the cement/metal interface. The bone cement[1] was hand-mixed at room temperature in the recommended ratios and kneaded for 10 s to allow air bubbles to release. An adequate volume of cement was placed within the prepared canal and the stem was then inserted using a dedicated fixture that ensured that the stem and bone axes were concentric and parallel. Following insertion, the cement mantle was pressurized for 5 min. to approximately 200 kPa (under axial compression), to minimize cement voids and to achieve uniform and complete interdigitation regardless of the bone surface topography. Pressures were determined by monitoring the load used in cement densification and dividing by the cement mantle cross-section. After pressurizing the bone cement was allowed to fully cure at room temperature.

The model THJR specimens were subjected to cyclic loads with a magnitude defined according to the room-temperature shear strength of the cement/bone interface. A sinusoidal load profile with a small reversal was chosen to simulate loads transmitted from the natural gait. According to De Santis et al. [27], the damping factor ($\tan\delta$ = ratio of loss modulus to storage modulus) of bone cement is almost equal for room and body temperature at 5 Hz. Consequently, all loading was applied using load control actuation with frequency of 5 Hz and at room temperature. While higher than natural gait, the frequency of loading was chosen to balance concerns related to the testing duration and potential frequency effects on the material

[1] ENDURANCE™ styrene copolymer bone cement donated by DePuy®

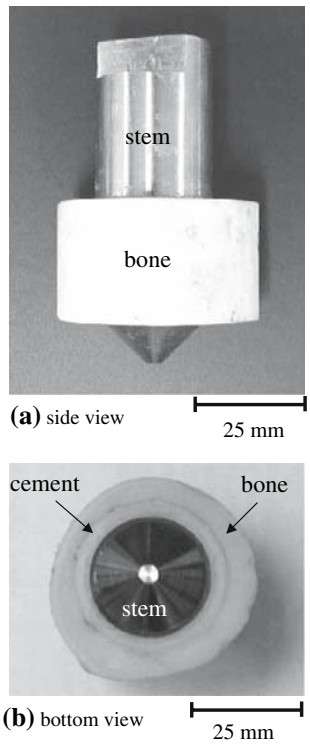

Fig. 2 A completed model THJR specimen. (**a**) Side view, (**b**) bottom view

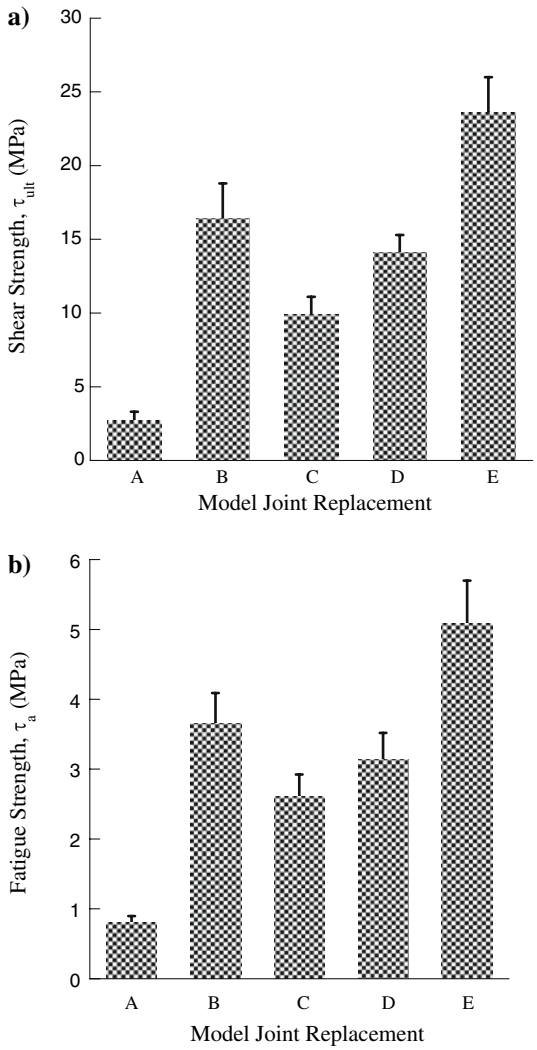

Fig. 3 Results from the pushout and fatigue tests conducted with the model THJR specimens. Details of the methods and results are given in Ref. [25]. The error bars indicate the standard deviation in strength for each group. (**a**) The shear strength of the cement/bone interface determined from pushout tests. (**b**) The fatigue strength of the cement/bone interface corresponding to a life of 10×10^6 cycles. Fatigue failure was defined by an absolute displacement between the cement and bone of 1 mm

behavior. The maximum cyclic load was chosen to achieve a maximum cyclic shear stress (τ_{max}) corresponding to 30%, 40% or 70% of the ultimate shear strength (τ_{ult}) of the interface, which was determined from pushout tests; results are summarized in Fig. 3a. A description of the methods used in evaluating τ_{ult} for the model implants is reported elsewhere [25]. A minimum cyclic stress (τ_{min}) of approximately 5% of the maximum stress was utilized to simulate forces of the abductor muscles during the swing phase of normal walking. According to the cyclic stress magnitude and load reversal used, the stress ratio was $R = -0.05$ where $R = \tau_{min}/\tau_{max}$. Fatigue loading was conducted using universal testing equipment and a specially designed fixture (Fig. 4a). Hydration of the specimens was maintained throughout cyclic loading using the calcium-buffered saline solution. The specimens were tested within 24 h to reduce the demineralization of bone. A stroke limit was defined to discontinue cyclic loading when the axial displacement reached 1 mm. The maximum period of evaluation was 500,000 cycles and was based upon the average number of steps a person takes a day over 6 months [28]. A total of 45 model hip replacement specimens were tested (5 tools and 3 specimens each at 3 load levels (30%, 40%, and 70% τ_{ult})).

Loosening was quantified in terms of the relative displacement (δ) that evolved between the stem and the bone with fatigue loading. The absolute displacement (δ_{abs}) was defined as the total displacement between the cement and the bone with respect to their positions in the first cycle (Fig. 4a). Preliminary results showed that δ_{abs} increased with number of load cycles (N) and that the displacement history exhibited 3 distinct regions of response (Fig. 4b); Regions I, II, and III corresponded to initial migration, steady state loosening and unstable loosening, respectively. The stress-life (τ–N) response was quantified in terms of the maximum cyclic shear stress and the number of cycles to a critical displacement. An empirical relationship was developed for the stress-life response of each group of model joint replacements according to

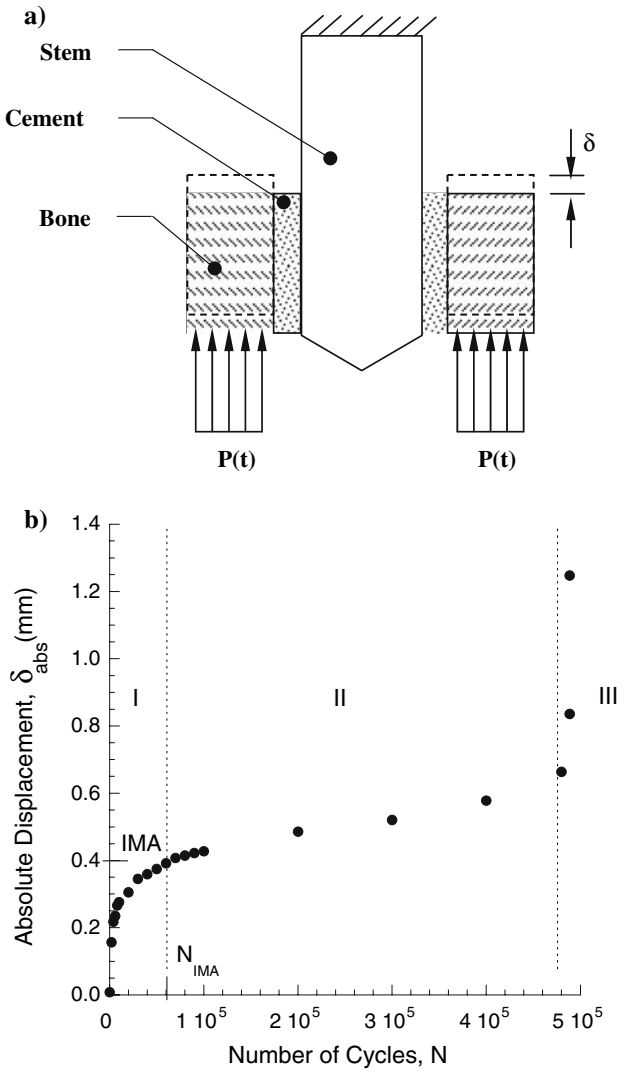

Fig. 4 Details of the cyclic load, measures of displacement and cyclic response used in characterizing loosening for the model implants. (**a**) Schematic diagram of the displacement associated with loosening (δ) and application of cyclic load ($P(t)$). (**b**) The three distinct regions of loosening evident from a typical absolute displacement (δ_{abs}) history. This response is for a 1-fluted specimen tested at 30% pushout strength

$$\tau_a = \alpha N^{\beta} \qquad [\text{MPa}] \tag{1}$$

where α and β are regarded as the fatigue strength coefficient and exponent, respectively, and N is the corresponding life (i.e., number of cycles evolved before reaching the critical displacement). The quantities α and β were determined for each bone surface preparation and were evaluated for a critical displacement of 1.0 mm. The apparent fatigue strength (τ_a) of the prepared cement/bone interfaces was estimated using Eq. 1 for a life of 10×10^6 cycles, which is equivalent to the average number of steps a person takes over a 10-year period. Results of the evaluation are presented in Fig. 3b and details have been reported elsewhere [25].

The surface texture of the prepared femoral canals was analyzed with a Hommel T8000 contact profilometer and a skid-type sensing probe with a 10 μm diameter diamond stylus. Profiles were obtained parallel to the canal using a traverse length of 15 mm and cutoff length of 2.5 mm. The average surface roughness (R_a) was calculated according to DIN 4762. Bearing height curves were constructed from surface profiles obtained from the femoral canals and used in estimating the core roughness (R_k), reduced peak height (R_{pk}), and reduced valley depth (R_{vk}) according to DIN 4776. The total volume available for cement interdigitation (V_i) within the bone topography was estimated over the profile traverse length per unit surface width according to [29]

$$V_i = \frac{R_{pk}(M_{r1})}{200} + \left(R_{pk} + \frac{R_k}{2}\right) \bullet \frac{(M_{r2} - M_{r1})}{100} + \left(R_{pk} + R_k + \frac{R_{vk}}{2}\right) \bullet \frac{(100 - M_{r2})}{100} \quad [\mu\text{m}] \tag{2}$$

where M_{r1}, M_{r2} are the peak and valley material ratios for the surface profile and were available from the bearing height curves. Sacrificial specimens from each group that were not subjected to fatigue loading were also prepared to examine the quality of cement interdigitation. The specimens subjected to fatigue were carefully sectioned, surface profiles of the cement and the bone were obtained, and the profiles were compared to those of the same surfaces prior to cyclic loading. The surface roughness measurements taken before (o) and after (f) failure were used to calculate the change in interdigitation volume (ΔV_i) according to

$$\Delta V_i = V_{i(o)} - V_{i(f)} \quad [\mu\text{m}]. \tag{3}$$

Significant differences were defined for ($p < 0.05$) and identified using the Students t-test. In addition, the failed specimens were also evaluated using a stereomicroscope.

3 Results

Typical surface profiles of the bone resulting from surface preparation are shown in Fig. 1. The R_a, core roughness parameters and V_i of the bone for each surface are listed in Table 1. In general, the femoral canal of specimens prepared with Tools A and E exhibited surface profiles that are nearly symmetric about the surface mean-line (i.e., Gaussian). In contrast, the surfaces prepared using Tools B–D exhibited asymmetric profile height distributions. Preparations with Tool B resulted in a negatively skewed surface while those resulting from use of Tools C and D

Table 1 Surface roughness parameters of the bone resulting from surface preparation

Surface/Tool	R_a (μm)	R_{pk} (μm)	R_k (μm)	R_{vk} (μm)	V_i (μm)
Tool A	5	9	13	15	17
Tool B	40	15	56	121	70
Tool C	46	130	59	15	132
Tool D	55	119	125	20	154
Tool E	111	28	297	102	219

resulted in a positively skewed surface. As evident from a comparison of the profiles, V_i, and surface roughness parameters, differences in the surface topography that affect interdigitation of cement cannot be quantified effectively using R_a.

Profiles of the cement mantle not subjected to fatigue appeared as reflections of the corresponding bone surfaces (Fig. 1). The surface roughness parameters for the cement mantles of each group of specimens are shown in Table 2. The R_a for the bone and cement of each group of specimens are within 6% except for the surface resulting from Tool A, which indicates that the cement was fully interdigitated within the interstices of the bone.

A surface profile obtained from the bone prepared with Tool C prior to fatigue loading is shown in Fig. 5a. Surface profiles obtained after fatigue failure are shown in Fig. 5b–d and correspond to specimens subjected to cyclic loading with maximum cyclic shear stress of 30%, 40%, and 70% of τ_{ult}, respectively. All the bone surfaces exhibited a reduction in peak-to-valley height with respect to that before fatigue loading (in Fig. 5a). The ΔV_i values estimated from the bone are listed in Table 3. A positive ΔV_i indicates that the V_i for cement decreased with fatigue due to changes in the profile height distribution of bone. The normalized change in ΔV_i was also estimated from the ratio of the average ΔV_i to V_i (Table 3). The femoral canal of specimens prepared with Tools A and E underwent the smallest change in V_i. The ΔV_i values of the cement surface profiles that resulted from fatigue loading are listed in Table 4. These changes in V_i are attributed to wear of the cement mantle with micromotion or failure of pieces of the bone

Table 2 Surface roughness parameters of the cement mantle after cementing of the model implants

Surface/Tool	R_a (μm)	R_{pk} (μm)	R_k (μm)	R_{vk} (μm)	V_i (μm)
Tool A	7	8	15	13	16
Tool B	37	88	56	13	90
Tool C	42	12	27	161	56
Tool D	53	9	94	140	90
Tool E	121	2	352	123	223

that become lodged in the cement. For some surfaces there was an increase in V_i for both the cement mantle and the bone surfaces after cyclic loading (Tables 3, 4). This suggests that wear of the cement occurred along the bone plateaus and that the cement particles collected within the valleys of the bone. In general, the surfaces produced with Tools B–D resulted in $\Delta V_i < 0$ indicating that the cement profile exhibited a larger volume for interdigitation of bone after cyclic loading. The overall smallest and largest changes in the surface profiles occurred to the specimens prepared with Tools A and E, respectively. Furthermore, the femoral canals prepared with Tools C and D showed the largest changes in the cement mantle profile as a result of cyclic loading.

Using the measures of V_i from the bone and the cement, the total interdigitation volumes for the cement/bone interfaces before and after fatigue loading were calculated and are listed in Table 5. The specimens with smallest changes in surface topography and interdigitation with loosening were prepared with Tool A. However, when evaluated in terms of the normalized V_i, the specimens with the smallest relative change in topography with fatigue were prepared using Tool E.

Cement debris was found on the bone side of the interfaces and most noticeable on the femoral canals of specimens prepared using Tool B. Typical features of the femoral canals from specimens subjected to cyclic stresses of 30% and 40% τ_{ult} are shown in Fig. 6a and b, respectively. Fractured particles of bone were identified in the cement mantles of the specimens prepared using Tools C and D (e.g., Fig. 7). Note that there is a large reduction in V_i for the specimens prepared using Tool C (Table 3), which is due to peaks of the bone that have fractured and are evident in Fig. 6. There were similar features in the cement mantles of specimens prepared using Tool D. Thus, preparation of the femoral canal and the corresponding surface topography are important to the generation and evolution of cement and bone debris.

The total change in interdigitation volume (ΔV_i (total)) was estimated from the bone and cement surfaces after fatigue and is plotted in terms of the volume of interdigitated cement that was estimated from the femoral canal surfaces (prior to fatigue) in Fig. 8. There is a decrease in total ΔV_i with interdigitation of cement. However, the specimens with lowest total ΔV_i were prepared using Tool A, i.e., the control specimens. Thus, increasing the extent of cement interdigitation is perhaps not the best method to reduce debris. These results indicate that the generation of debris is dependent on the volume of interdigitation and the shape of the surface topography. Though difficult to make definitive statements, surfaces with low R_a and V_i or high R_a and V_i appeared to be effective at minimizing development of interface debris.

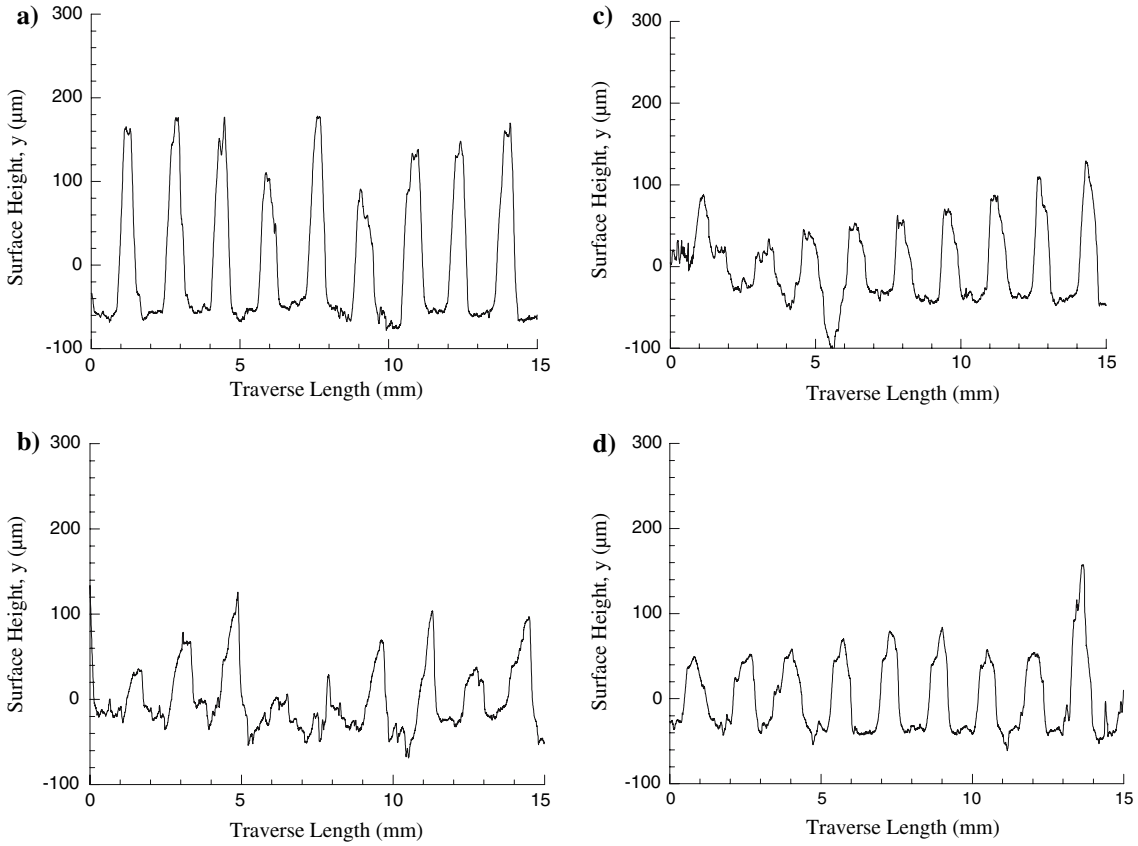

Fig. 5 Comparison of surface profiles of bone resulting from preparation of the femoral canal using Tool C. The profiles in (**b**) and (**c**) failed due to loosening of the stem of 1.0 mm within the specified number of cycles (N_f). (**a**) Bone surface before cyclic loading. R_a = 46 μm. (**b**) Bone surface after failure (N_f = 385,000 cycles) that was subjected to cyclic loading with τ_{max} = 40% τ_{ult}. R_a = 31 μm. (**c**) Bone surface after failure (N_f = 251,000 cycles) subjected to cyclic loading with τ_{max} = 30% τ_{ult}. R_a = 32 μm. (**d**) Bone surface after failure (N_f = 631 cycles) subjected to cyclic loading with τ_{max} = 70% τ_{ult}. R_a = 33 μm

Table 3 The change in interdigitation volume for cement estimated from the bone surface profiles after fatigue failure. Items with different letters are significantly different

Surface/Tool	ΔV_i (μm) τ_{max} = 30% τ_{ult}	ΔV_i (μm) τ_{max} = 40% τ_{ult}	ΔV_i (μm) τ_{max} = 70% τ_{ult}	$\left\lvert\frac{\Delta V_i}{V_i}\right\rvert_{Avg} \times 100\%$
Tool A	–1 ± 0 a	–2 ± 1 a	2 ± 1 a	10
Tool B	–25 ± 4 b	–31 ± 3 b	–7 ± 2 b	30
Tool C	94 ± 7 c	80 ± 9 d	71 ± 7 d	62
Tool D	28 ± 2 b	48 ± 1 c	74 ± 6 d	32
Tool E	–3 ± 1 a	42 ± 3 c	21 ± 3 c	10

Table 4 The change in interdigitation volume for bone estimated from the cement surface profiles after fatigue failure. Items with different letters are significantly different

Surface/Tool	ΔV_i (μm) τ_{max} = 30% τ_{ult}	ΔV_i (μm) τ_{max} = 40% τ_{ult}	ΔV_i (μm) τ_{max} = 70% τ_{ult}	$\left\lvert\frac{\Delta V_i}{V_i}\right\rvert_{Avg} \times 100\%$
Tool A	4 ± 2 a	1 ± 0 a	2 ± 1 a	15
Tool B	–41 ± 5 b	–15 ± 2 b	–57 ± 5 c	42
Tool C	–27 ± 6 b	–37 ± 6 c	–30 ± 4 b	56
Tool D	–1 ± 1 a	–15 ± 3 b	3 ± 1 a	7
Tool E	8 ± 4 a	–11 ± 2 b	7 ± 1 a	4

Table 5 The total volume of interdigitation for the cement/bone interface estimated from the interface profiles before fatigue and fatigue failure

Surface/Tool	V_i total (μm) Before fatigue	V_i total (μm) After fatigue	$\frac{\Delta V_i}{V_i} \times 100\%$
Tool A	33	30	8
Tool B	160	219	–36
Tool C	188	137	27
Tool D	244	198	19
Tool E	441	420	5

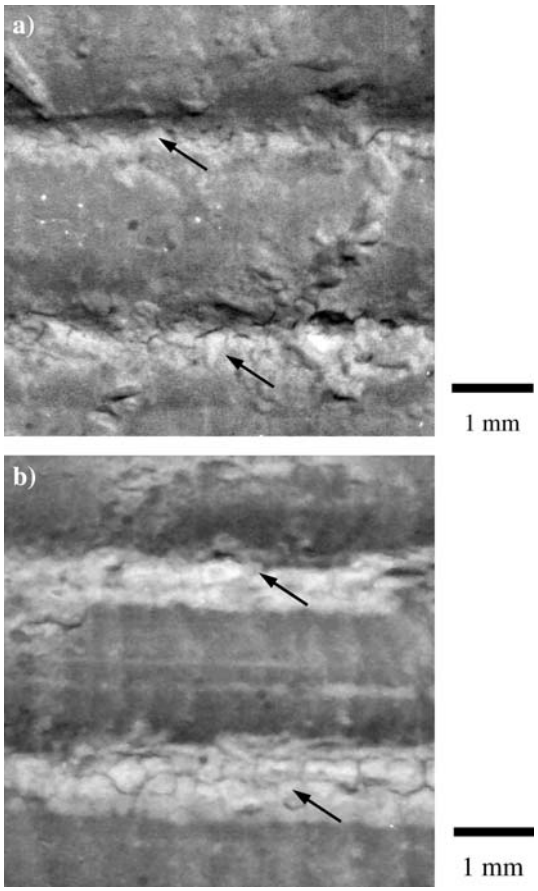

Fig. 6 Examples of the femoral canal surface of the model THJR specimens prepared with Tool B after fatigue failure. Note the presence of cement debris in the valleys of the surface as highlighted by the arrows. (**a**) Femoral canal (bone) surface of specimen after fatigue failure (δ_{abs} = 1 mm) τ_{max} = 30% τ_{ult}; N_f = 299,000 cycles. (**b**) Femoral canal (bone) surface of specimen after fatigue failure (δ_{abs} = 1 mm) τ_{max} = 40% τ_{ult}; N_f = 25,000 cycles

4 Discussion

Results of the experimental evaluation showed that both the pushout strength and the fatigue strength of the model THJR specimens were dependent on V_i of the cement (Fig. 3a, and b, respectively). In general, both the pushout strength and apparent fatigue strength increased proportionally with an increase in V_i [25]. However, in comparing the strength of the interfaces with the change in interdigitation volume with cyclic loading there was no correlation. Surfaces that exhibited the largest fatigue strength did not undergo the smallest changes in the interface geometry. Furthermore, there was also no correlation between the apparent rate of loosening and the changes in the interface geometry.

Both the bone and the cement surfaces along the cement mantle underwent significant topographical changes as a result of cyclic loading. While the volume of wear debris

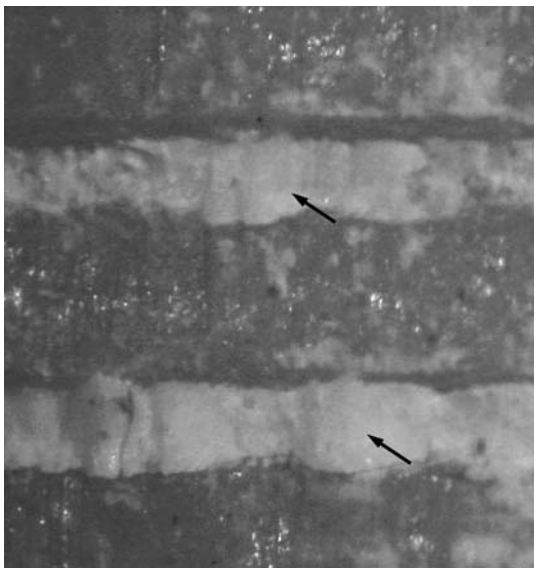

Fig. 7 Example of the cement mantle surface of a specimen prepared with Tool C after fatigue failure (δ_{abs} = 1 mm) τ_{max} = 30% τ_{ult}; N_f = 385,000 cycles

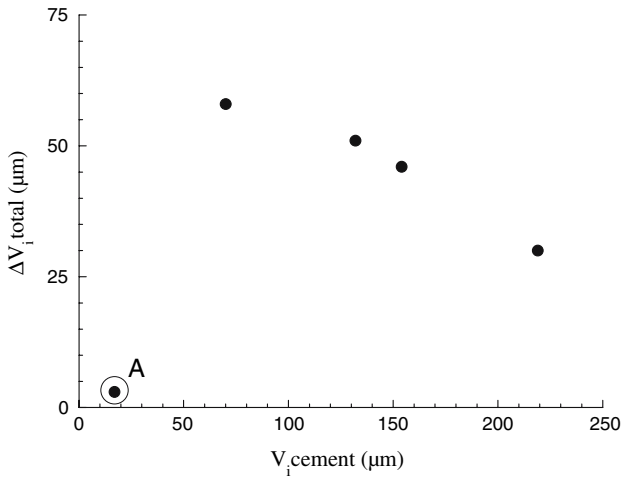

Fig. 8 The influence of cement interdigitation cement on changes in the interdigitation volume with fatigue loading. The control surface is circled in this graph

was not measured directly, quantitative measures of the surface topography revealed that there were changes that would undoubtedly result in the generation of debris. There were also significant differences in the ΔV_i between some of the groups with unique femoral canal surface preparations. It is generally believed that the development of cement debris at the cement/bone interface is a result of inadequate interdigitation of cement [30]. However, the largest changes in the interface geometry occurred to the specimens with intermediate volume of interdigitation (prepared using Tools B–D). In most cases, the ΔV_i for these specimens was significantly larger than that obtained for specimens prepared with Tools A and E. It is important to emphasize that the study was limited to a maximum of 500 kcycles and corresponds to the first 6 months post-surgery. While interface debris developed within this period may contribute to the transition from early migration to clinical loosening [31], there may be unique changes in the interface geometry with additional cyclic loading.

The model THJR specimens were prepared using dense cortical bone from the mid-diaphyseal region of bovine femurs. As such, interdigitation of cement was limited to the interstices of the machined surfaces. In most cemented total joint replacements, mechanical interlock is achieved through interdigitation of cement within the cancellous bone. In these instances the volume fraction of interdigitated cement may be greater than that achieved within specially prepared cortical bone. The ratio of bone to cement within the interdigitated region is an important concept. The influence of the volume fraction of interdigitated cement on the change in interdigitation of cement with loosening is shown in Fig. 9a. The smallest changes in the cement occurred for the specimens with nearly equal volume fractions of cement and bone within the hybrid zone (V_f (cement) = 0.5). Similarly, the change in interdigitation of bone with cyclic loading in terms of the volume fraction of interdigitated bone is shown in Fig. 9b. According to these results, the optimum volume fraction of cement within the hybrid zone for minimizing the development of debris is near 0.5. This suggestion ignores the potential differences related to the quality of porous bone and the difficulty in achieving interdigitation. For instance, the relative porosity of cancellous bone has a significant influence on the bone strength [32, 33] and may have an effect on the optimum cement to bone ratio.

There are several limitations to this study. The model THJR specimens were subjected to constant-amplitude cyclic loads at 5 Hz that resulted in pure shear loading of the interface. A THJR is subjected to complicated spectrum cyclic loading with frequency closer to 1 Hz and the cement/bone interface in vivo is subjected to a combination of normal and shear stresses. A reduction in the frequency of loading would be expected to lower the

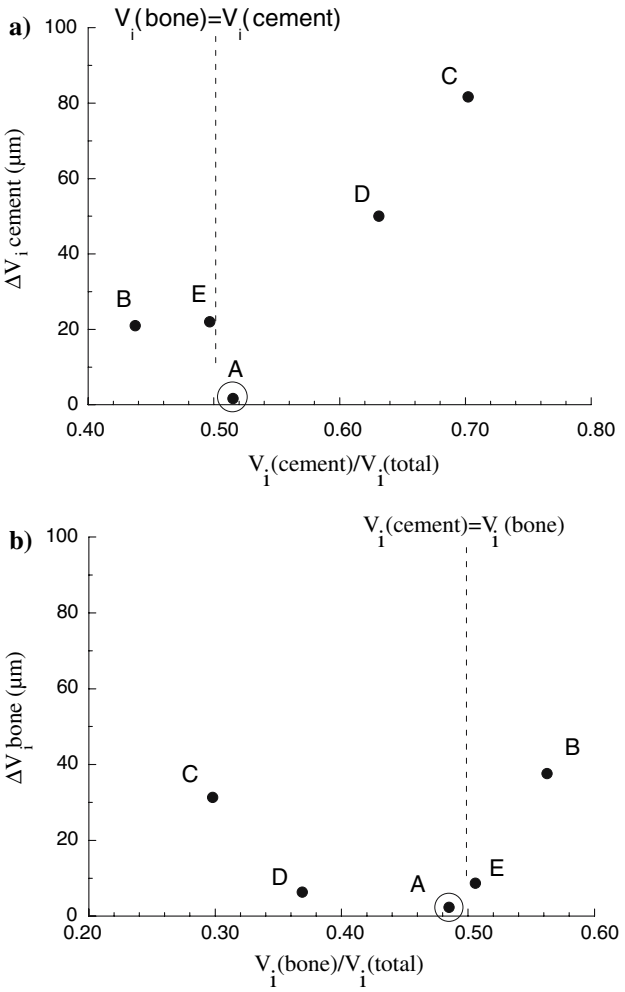

Fig. 9 The influence of interdigitation on changes to the cement/bone interface with cyclic loading. The control surface is circled in both graphs. (**a**) The influence of the volume of interdigitation of cement on the change in interdigitation of cement with cyclic loading. (**b**) The influence of the volume of interdigitation of bone on the change in interdigitation of bone with cyclic loading

apparent fatigue strength due to contributions from viscoelastic/viscoplastic deformation to loosening and degradation of the interface. Also, the in vitro evaluation did not account for biological factors or enable potential synergistic responses. Future studies should be conducted to evaluate the contribution of the surface topography of the bone to the biological aspects of the interface response. In the interest of examining a relatively wide range of surfaces, only three specimens were tested for each surface preparation and stress range. An investigation involving a larger number of specimens and treatments could provide a more detailed understanding. Finally, mechanical interlock between the bone and cement was achieved exclusively through interdigitation of cement within cortical bone whereas interdigitation is more often achieved within cancellous bone. Variations in these aspects of the bone

would undoubtedly affect the interface behavior under fatigue and is an important concern that remains to be addressed. It is expected that results from the present study will provide a valuable benchmark for future studies that examine fatigue properties of the cement/bone interface involving trabecular bone.

5 Conclusions

An experimental study was conducted to examine loosening of the cement/bone interface and development of interfacial wear debris that results from cyclic loading. Based on the results from this study, the following conclusions were drawn.

1. Fatigue loading resulted in changes in the surface morphology of both the cement and bone due to interfacial wear. The nature of changes depended on the initial surface topography of the machined femoral canal.
2. Debris generation was largely a function of the surface topographies of the bone and the cement mantle. There was a reduction in the volume of cement debris with an increase in the interdigitation of cement within the bone. However, the model THJR specimens with the lowest volume of debris also had the lowest volume of cement interdigitation. Bone surfaces with symmetric profile height distribution (i.e., Gaussian) resulted in the lowest volume of wear debris.
3. There was no correlation between the apparent fatigue strength of the cement/bone interface and the change in volume of interdigitation that occurred with cyclic loading. Surfaces that exhibited the largest fatigue strength did not result in the smallest volume of wear debris.
4. When properties of the cement/bone interface associated with fatigue loading were evaluated in terms of the volume fraction of cement (V_f(cement)), a V_f(cement) of 0.5 was found to be the optimum and resulted in the minimum volume of debris.

Acknowledgements Support for this study was provided through a grant from the Maryland Chapter of the Arthritis Foundation.

References

1. D. J. BERRY, *J. Arthroplasty* **19** (2004) 83
2. R. C. GARDINER and W. J. HOZACK, *J. Bone Joint Surg.* **76B** (1994) 49
3. C. G. MOHLER, J. J. CALLAGHAN, D. K. COLLIS and R. C. JOHNSTON, *J. Bone Joint Surg.* **77A** (1995) 1315
4. D. G. KIM, M. A. MILLER and K. A. MANN, *J. Biomech.* **37** (2004) 1505
5. D. G. KIM, M. A. MILLER and K. A. MANN, *J. Orthop. Res.* **22** (2004) 633
6. H. G. WILLERT, H. BERTRAM and G. H. BUCHHORN, *Clin. Orthop.* **258** (1990) 108
7. M. JASTY, W. JIRANEK and W. H. HARRIS, *Clin. Orthop.* **285** (1992) 116
8. L. C. JONES, C. FRONDOZA and D. S. HUNGERFORD, *J. Bone Joint Surg.* **83B** (2001) 448
9. J. A. WIMHURST, R. A. BROOKS and N. RUSHTON, *J. Bone Joint Surg.* **83B** (2001) 588
10. W. J. MALONEY, M. JASTY, A. ROSENBERG and W. H. HARRIS, *J. Bone Joint Surg.* **72B** (1990) 966
11. M. J. JASTY, W. E. FLOYD III, A. L. SCHILLER, S. R. GOLDRING and W. H. HARRIS, *J. Bone Joint Surg.* **68A** (1986) 912
12. D. D. GOETZ, E. J. SMITH and W. H. HARRIS, *J. Bone Joint Surg.* **76A** (1994) 1121
13. M. KRISMER, R. BIEDERMANN, B. STÖCKL, M. FISCHER, R. BAUER and C. HAID, *J. Bone Joint Surg.* **81B** (1999) 273
14. A. KOBAYASHI, W. J. DONNELLY, G. SCOTT and M. A. FREEMAN, *J. Bone Joint Surg.* **79B** (1997) 583
15. M. A. FREEMAN and P. PLANTE-BORDENEUVE, *J. Bone Joint Surg.* **76B** (1994) 432
16. J. KÄRRHOLM, B. BORSSEN, G. LOWENHIELM and F. SNORRASON, *J. Bone Joint Surg.* **76B** (1994) 912
17. P. ASPENBURG and H. VAN DE VIS, *Clin. Orthop.* **352** (1998) 75
18. K. A. MANN, D. C. AYERS, F. W. WERNER, R. J. NICOLETTA and M. D. FORTINO, *J. Biomech.* **30** (1997) 339
19. R. D. CROWNINSHIELD, J. D. JENNINGS, M. L. LAURENT and W. J. MALONEY, *Clin. Orthop.* **355** (1998) 90
20. R. HUISKES, N. VERDONSCHOT and B. NIVBRANT, *Clin. Orthop.* **355** (1998) 103
21. K. A. MANN, F. W. WERNER and D. C. AYERS, *J. Biomech.* **32** (1999) 1251
22. N. VERDONSCHOT and R. HUISKES, *Clin. Orthop.* **329** (1996) 326
23. D. J. BEAN, F. R. CONVERY, S. L.-Y. WOO and R. L. LIEBER, *J. Arthroplasty* **2** (1987) 293
24. K. G. HEIPLE, K. L. SHEA, D. L. NELSON and D. T. DAVY, in Transactions of the 32nd Orthop. Res. Soc. (New Orleans, LA, 1986), p. 354
25. D. AROLA, K. A. STOFFEL and D. T. YANG, *J. Biomed. Mater. Res. Appl Biomater.* **76** (2006) 287
26. M. B. GUSTAFSON, G. W. MARTIN, V. GIBSON, D. H. STORMS, S. M. STOVER, J. GIBELING and L. GRIFFIN, *J. Biomech.* **29** (1996) 1191
27. R. DE SANTIS, F. MOLLICA, L. AMBROSIO, L. NICOLAIS and D. RONCA, *J. Mater. Sci. Mater. Med.* **14** (2003) 583
28. M. MORLOCK, E. SCHNEIDER, A. BLUHM, M. VOLLMER, G. BERGMANN, V. MULLER and M. HONL, *J. Biomech.* **34** (2001) 873
29. D. AROLA, D. T. YANG and K. A. STOFFEL, *J. Biomed. Mater. Res. Appl. Biomater.* **58** (2001) 519
30. G. H. ISAAC, B. M. WROBLEWSKI, J. R. ATKINSON and D. DOWSON, *Clin. Orthop.* **276** (1992) 115
31. K. A. MANN, M. J. ALLEN and D. C. AYERS, *J. Orthop. Res.* **16** (1998) 370
32. N. L. FAZZALARI, M. R. FORWOOD, K. SMITH, B. A. MANTHEY and P. HERREEN, *Bone* **22** (1998) 381
33. T. M. KEAVENY, F. F. MORGAN, G. L. NIEBUR and O. C. YEH, *Annu. Rev. Biomed. Eng.* **3** (2001) 307